논문 21-46-08-12 The Journal of Korean Institute of Communications and Information Sciences '21-08 Vol.46 No.08
https://doi.org/10.7840/kics.2021.46.8.1301

Comparison of Different Wavelengths for Estimating HbA1c and SpO_2 Noninvasively Using Beer-Lambert Law and Photon Diffusion Theory Derived Models

Shifat Hossain◆, Ki-Doo Kim°

ABSTRACT

Photoplethysmography (PPG) is a widely used method for detecting the blood volume changes in the limbs of human body using different wavelengths of light. Many physiological parameters are estimated through the use of the PPG signals in recent studies including glycated hemoglobin (HbA1c) and blood oxygenation (SpO2). However, the processes of estimating the physiological parameters are dependent on the wavelengths of light used to acquire the PPG signal. In this study, we compare wavelengths from 300nm to 1100nm for four models to estimate HbA1c and SpO2 levels with higher accuracy. These four models were constructed from Beer-Lambert and photon diffusion theories. From the analyses of 300nm to 1100nm, it is seen that the best sets of wavelengths are found to be {426nm, 721nm, 1100nm} and {426nm, 678nm, 1100nm} for two Beer-Lambert based models, respectively. On the other hand, for both of the photon diffusion-based models, the {426nm, 384nm, 1100nm} set is found to be the best performing wavelengths. Moreover, from the analysis of the six widely used wavelengths in different PPG systems, the {465nm, 525nm, 660nm} is found to be the best performing set of wavelengths that results in higher accuracy for HbA1c and SpO2 estimation using all four models.

Key Words : Photoplethysmography, Wavelength selection, HbA1c, SpO2, Beer-Lambert, Photon-Diffusion

Ⅰ. Introduction

Photoplethysmography (PPG) is a method to detect blood volume changes in the subcutaneous tissues of the peripheries (i.e. fingertip, earlobe, esophagus, etc.). This is a non-invasive optical method to obtain plethysmogram. In PPG, the tissues of the epidermis are illuminated with different numbers and wavelengths of light sources, and the plethysmogram is obtained by placing a photodetector (PD) in the same plane with the LEDs to detect the light reflected by cellular reflectors and scattering in the skin (reflection type PPG) or PD placed at a distance of the organ thickness and the transmitted light is monitored (transmission type PPG). The most common type of PPG is the transmission type fingertip PPG. In most of the PPG researches, fingertip and earlobe PPG systems have been used, which can be both transmission and reflection types[1,2]. For sports/exercise tracking systems, commercially, the reflection type wrist PPG system is very popular since it is designed within a wristwatch/band for design convenience[3].

PPG systems are used in widely varied

※ This research was supported by the National Research Foundation of Korea Grant funded by the Ministry of Science, ICT, Future Planning [2015R1A5A7037615].
※ Was also results of a study on the "Leaders in INdustry-university Cooperation +" Project, supported by the Ministry of Education and National Research Foundation of Korea.
◆ First Author : Kookmin University Department of Electronics Engineering, shifathosn@kookmin.ac.kr, 학생회원
° Corresponding Author : Kookmin University Department of Electronics Engineering, kdk@kookmin.ac.kr, 종신회원
논문번호 : 202106-138-C-RE, Received June 21, 2021; Revised August 4, 2021; Accepted August 9, 2021

applications. These applications can be widely categorized into two types - blood element measurements and physiological measurements. The blood element measurement systems estimate the amount (in volumes or percentage) of elements of blood, i.e. "Blood Oxygenation" or "Pulse Oximetry"[4], "Blood Glucose measurement"[5,6], "Glycated Hemoglobin estimation"[7], "Hypo- and Hypervolemia estimation"[8] measuring the percentage amount of Oxygenated Hemoglobin, per-volume amount of glucose dissolved in blood plasma and overall blood volume present in human body respectively. And the physiological measurements include heart rate monitoring[9], respiration[10], depth of anesthesia[11], blood pressure[12], etc.

In all these applications, one or more light sources are used to estimate the blood elements and physiological measurements. And these light sources are selected mostly based on the personal preferences of the researchers. The commercially available PPG devices mostly utilize the Red and IR light sources for estimation of heart rate and blood oxygenation. However, in research and studies of different applications of PPG, Blue[7], Green[6,7,10,13], Yellow[13], Orange[14], Red[4,6,7], and IR[4,6] have been used.

In this study, we compare the different light sources for estimating glycated hemoglobin (HbA1c) and blood oxygenation (SpO_2) levels. We have deduced four mathematical fingertip models. And then after the construction of the models the range of the light sources tested is from 300nm to 1100nm.

Ⅱ. Methodology

To compare among a different set of wavelengths for estimating HbA1c and SpO_2 values for Beer-Lambert and photon diffusion model, we first need to construct the models using different model assumptions. We are using three wavelengths to estimate the glycated hemoglobin and blood oxygenation levels. The Beer-Lambert and photon-diffusion-based models are also designed to estimate the target parameters with these three wavelengths of light. The construction process of the models is given in the following sections.

2.1 Beer-Lambert Model

The Beer-Lambert law states, the absorbance of a solution having N number of attenuating components as in (1),

$$A = C_a d = -\log\left(\frac{I}{I_0}\right) \approx \sum_{i=1}^{N} \epsilon_i(\lambda) \times c_i \times d \tag{1}$$

where A, C_a, ϵ, c, and d denote absorptivity, absorption coefficient, molar attenuation coefficient, concentration, and length of the light beam in the solution. The last expression in (1) is true only for a homogenous solution where the attenuation is uniform throughout the whole solution.

2.2 Blood-Vessel Model

Now, if we consider the blood components as the oxyhemoglobin (HbO), deoxyhemoglobin (HHb) and glycated hemoglobin (HbA1c), the equation (1) can be written as follows,

$$\begin{aligned} A &= \left(\epsilon_a^{HbA1c}(\lambda) \times c_{HbA1c} + \epsilon_a^{HbO}(\lambda) \times c_{HbO} + \epsilon_a^{HHb}(\lambda) \times c_{HHb}\right) \times d \\ &= -\log\left(\frac{I}{I_0}\right) \end{aligned} \tag{2}$$

The molar absorption coefficients of HbA1c were taken from studies by Hossain, S. et al.[15], and absorption coefficients of HbO and HHb were taken from Prahl, S.A.[16], respectively. Now, we let the d change due to the change in blood volume in blood vessel. So, we can write,

$$\delta A = \left(\epsilon_a^{HbA1c}(\lambda) \times c_{HbA1c} + \epsilon_a^{HbO}(\lambda) \times c_{HbO} + \epsilon_a^{HHb}(\lambda) \times c_{HHb}\right) \times \delta d \tag{3}$$

For, three wavelengths of light (λ_1, λ_2, and λ_3), this equation (3) can be defined for three λ values resulting in $\delta A_{\lambda 1}$, $\delta A_{\lambda 2}$, and $\delta A_{\lambda 3}$. Now from these equations, we can construct the ratio equation as follows,

$$R_1 = \frac{\delta A_{\lambda 1}}{\delta A_{\lambda 3}} = \frac{\epsilon_a^{HbA1c}(\lambda_1) \times c_{HbA1c} + \epsilon_a^{HbO}(\lambda_1) \times c_{HbO} + \epsilon_a^{HHb}(\lambda_1) \times c_{HHb}}{\epsilon_a^{HbA1c}(\lambda_3) \times c_{HbA1c} + \epsilon_a^{HbO}(\lambda_3) \times c_{HbO} + \epsilon_a^{HHb}(\lambda_3) \times c_{HHb}} \tag{4}$$

$$R_2 = \frac{\delta A_{\lambda 2}}{\delta A_{\lambda 3}} = \frac{\epsilon_a^{HbA1c}(\lambda_2)\times c_{HbA1c} + \epsilon_a^{HbO}(\lambda_2)\times c_{HbO} + \epsilon_a^{HHb}(\lambda_2)\times c_{HHb}}{\epsilon_a^{HbA1c}(\lambda_3)\times c_{HbA1c} + \epsilon_a^{HbO}(\lambda_3)\times c_{HbO} + \epsilon_a^{HHb}(\lambda_3)\times c_{HHb}} \quad (5)$$

and

$$R_3 = \frac{\delta A_{\lambda 1}}{\delta A_{\lambda 2}} = \frac{\epsilon_a^{HbA1c}(\lambda_1)\times c_{HbA1c} + \epsilon_a^{HbO}(\lambda_1)\times c_{HbO} + \epsilon_a^{HHb}(\lambda_1)\times c_{HHb}}{\epsilon_a^{HbA1c}(\lambda_2)\times c_{HbA1c} + \epsilon_a^{HbO}(\lambda_2)\times c_{HbO} + \epsilon_a^{HHb}(\lambda_2)\times c_{HHb}} \quad (6)$$

Now we are defining partial concentration of oxyhemoglobin and glycated hemoglobin as follows,

$$P_{HbO} = \frac{c_{HbO}}{c_{HHb} + c_{HbO} + c_{HbA1c}} \quad (7)$$

$$P_{HbA1c} = \frac{c_{HbA1c}}{c_{HHb} + c_{HbO} + c_{HbA1c}} \quad (8)$$

Applying (7)-(8) in (4), (5), and (6), we get,

$$R_1 = \frac{P_{HbA1c}\left(\epsilon^{HbA1c}(\lambda_1) - \epsilon^{HHb}(\lambda_1)\right) + P_{HbO}\left(\epsilon^{HbO}(\lambda_1) - \epsilon^{HHb}(\lambda_1)\right) + \epsilon^{HHb}(\lambda_1)}{P_{HbA1c}\left(\epsilon^{HbA1c}(\lambda_3) - \epsilon^{HHb}(\lambda_3)\right) + P_{HbO}\left(\epsilon^{HbO}(\lambda_3) - \epsilon^{HHb}(\lambda_3)\right) + \epsilon^{HHb}(\lambda_3)} \quad (9)$$

$$R_2 = \frac{P_{HbA1c}\left(\epsilon^{HbA1c}(\lambda_2) - \epsilon^{HHb}(\lambda_2)\right) + P_{HbO}\left(\epsilon^{HbO}(\lambda_2) - \epsilon^{HHb}(\lambda_2)\right) + \epsilon^{HHb}(\lambda_2)}{P_{HbA1c}\left(\epsilon^{HbA1c}(\lambda_3) - \epsilon^{HHb}(\lambda_3)\right) + P_{HbO}\left(\epsilon^{HbO}(\lambda_3) - \epsilon^{HHb}(\lambda_3)\right) + \epsilon^{HHb}(\lambda_3)} \quad (10)$$

$$R_3 = \frac{P_{HbA1c}\left(\epsilon^{HbA1c}(\lambda_1) - \epsilon^{HHb}(\lambda_1)\right) + P_{HbO}\left(\epsilon^{HbO}(\lambda_1) - \epsilon^{HHb}(\lambda_1)\right) + \epsilon^{HHb}(\lambda_1)}{P_{HbA1c}\left(\epsilon^{HbA1c}(\lambda_2) - \epsilon^{HHb}(\lambda_2)\right) + P_{HbO}\left(\epsilon^{HbO}(\lambda_2) - \epsilon^{HHb}(\lambda_2)\right) + \epsilon^{HHb}(\lambda_2)} \quad (11)$$

Using these (9), (10), and (11), we can calculate the concentration of HbA1c and SpO_2 for three wavelengths of light.

2.3 Whole-Finger Model

The previous model assumptions only consider blood contents, which is a very rough estimate of the actual fingertip elements. To have a more accurate representation of fingertip, we can also define the blood components with the fingertip skin and water contents for a more realistic model definition as follows,

$$C_a = \left(V_a\mu_a^{art}(\lambda) + V_v\mu_a^{vein}(\lambda) + V_w\mu_a^{water}(\lambda) + [1-(V_a+V_v+V_w)]\mu_a^{baseline}\right)\times d \quad (12)$$

$$where, \mu_a^{art} = \mu_a^{HHb} + P_{HbO}^{art}\left(\mu_a^{HbO} - \mu_a^{HHb}\right) + P_{HbA1c}^{art}\left(\mu_a^{HbA1c} - \mu_a^{HHb}\right) \quad (13)$$

$$\mu_a^{vein} = \mu_a^{HHb} + P_{HbO}^{vein}\left(\mu_a^{HbO} - \mu_a^{HHb}\right) + P_{HbA1c}^{vein}\left(\mu_a^{HbA1c} - \mu_a^{HHb}\right) \quad (14)$$

Here, the C_a is the absorption coefficient of the fingertip model. The V_a, V_v, and V_w are the partial volume fractions of the artery, vein, and water, respectively. The terms with μ indicate the absorption coefficient of the respective element. The superscript "art" and "vein" indicate the properties of the artery and vein, respectively. Moreover, the baseline absorption coefficient indicates the absorption coefficient of dermal layers.

Now from (12), we can assume that incoming blood at the artery will cause a change (ΔV_a) in the partial volume of the arterial composition resulting in a change (ΔC_a) in the absorption coefficient. This results in

$$C_a + \Delta C_a = (V_a + \Delta V_a)\mu_a^{art}(\lambda) + V_v\mu_a^{vein}(\lambda) + V_w\mu_a^{water}(\lambda) + [1-(V_a+\Delta V_a+V_v+V_w)]\mu_a^{baseline} \quad (15)$$

Now, subtracting (12) from (15), we get

$$\Delta C_a = \Delta V_a\left(\mu_a^{art}(\lambda) - \mu_a^{baseline}(\lambda)\right) \quad (16)$$

From (1) we get

$$I = I_0\ 10^{-C_a d} \quad (17)$$

Differentiating (17) with respect to C_a, we get

$$\frac{dI}{dC_a} = -\ln(10) I_0 d\ 10^{-C_a d} \approx \frac{\Delta I}{\Delta C_a} \quad (18)$$

So, from (18) we get

$$\Delta I \approx -\ln(10) I_0 \Delta C_a d\ 10^{-C_a d} \quad (19)$$

Now, replacing ΔC_a in (19) from (16) and dividing by (17) we get

$$\frac{\Delta I}{I} = -\ln(10)\Delta V_a\left(\mu_a^{art}(\lambda) - \mu_a^{baseline}(\lambda)\right)d \quad (20)$$

Thus, we can define the ratio equations for this model assumption as follows.

$$R_1 = \frac{\left[\frac{\Delta I}{I}\right]_{\lambda 1}}{\left[\frac{\Delta I}{I}\right]_{\lambda 3}} = \frac{\mu_a^{art}(\lambda_1) - \mu_a^{baseline}(\lambda_1)}{\mu_a^{art}(\lambda_3) - \mu_a^{baseline}(\lambda_3)} \quad (21)$$

$$R_2 = \frac{\left[\frac{\Delta I}{I}\right]_{\lambda 2}}{\left[\frac{\Delta I}{I}\right]_{\lambda 3}} = \frac{\mu_a^{art}(\lambda_2) - \mu_a^{baseline}(\lambda_2)}{\mu_a^{art}(\lambda_3) - \mu_a^{baseline}(\lambda_3)} \quad (22)$$

$$R_3 = \frac{\left[\frac{\Delta I}{I}\right]_{\lambda 1}}{\left[\frac{\Delta I}{I}\right]_{\lambda 2}} = \frac{\mu_a^{art}(\lambda_1) - \mu_a^{baseline}(\lambda_1)}{\mu_a^{art}(\lambda_2) - \mu_a^{baseline}(\lambda_2)} \quad (23)$$

From (21)-(23), the glycated hemoglobin and blood oxygenation levels can be estimated using the whole-finger model assumptions. These two models mentioned above are described in [7].
where,

$$K_r(\alpha,\ r) = \frac{-r^2}{1+\alpha r}$$

Using these ratio equations (33)-(35) and (36)-(38) for transmission and reflective type PPG systems, respectively, the glycated hemoglobin and blood oxygenation parameters can be estimated.

2.4 Ratio Equations Analysis

All four of the models described above result in a set of ratio equations. All these ratio equations are a function of two wavelengths, blood oxygenation, and glycated hemoglobin parameters. So, for each set of wavelengths (λ_1, λ_2, λ_3) we can get the ratio equations dependent only on HbA1c and SpO_2 terms.

$$R = f(SpO_2,\ HbA1c) \quad (39)$$

Now, differentiating this equation with respect to HbA1c and SpO_2, we can get $\frac{dR}{dHbA1c}$ and $\frac{dR}{dSpO_2}$, respectively.

Now, we can have the arithmetic mean of the two expressions mentioned above as follows.

$$M_h = \frac{\sum_{i=1}^{3} \frac{dR_i}{dHbA1c}}{3} \quad (40)$$

$$M_s = \frac{\sum_{i=1}^{3} \frac{dR_i}{dSpO_2}}{3} \quad (41)$$

Now, having the largest value of M_h and M_s for each set of wavelengths of light is defined to have much more sensitivity to the change of the respective parameters (HbA1c and SpO_2). So, having a higher value of M_h and M_s can as a result indicate the best set of wavelengths for a given model for estimating a specific parameter.

Ⅲ. Results and Discussion

The M_h and M_s metrics derived in the previous section are dependent on the change of HbA1c and SpO_2 parameter values. The higher the change of the

Table 1. Analysis results for the best set of wavelengths for each model and each parameter.

Model	M_h	Wavelength set for HbA1c (nm)	M_s	Wavelength set for SpO^2 (nm)
Beer-Lambert Blood-vessel model	31.26	{426, 721, 1100}	31.26	{426, 721, 1100}
Beer-Lambert Whole-finger model	44.93	{426, 678, 1100}	44.93	{426, 678, 1100}
Photon-diffusion Transmission model	17.18	{426, 384, 1100}	17.18	{426, 384, 1100}
Photon-diffusion Reflection model	26.73	{426, 384, 1100}	26.73	{426, 384, 1100}

ratio values depending on the change of the previously mentioned parameters (HbA1c and SpO_2) for a specific set of wavelengths, it can be said that the sensitivity of the parameters at that wavelength set is higher, hence resulting in higher estimation accuracy if that wavelength set is used.

Analyzing the ratio equations from different models described in the previous section with (40) and (41), we can derive the set of wavelengths that have the maximum M_h and M_s values. In Table 1, we have shown the set of wavelengths having the maximum value of M_h and M_s for each specific model.

The values of M_h and M_s for each set of wavelengths can be illustrated in 3-dimensional plots, each axis representing a wavelength. The following figure illustrates the M_h values for all the possible wavelength combinations.

From Fig. 1 we can see that all the models exhibit a similar pattern, but the patterns of the Beer-Lambert-based models have a very high slope with the slightest change in the selection of wavelengths. On the other hand, the photon diffusion-based models exhibit smooth flow of pattern in the wavelength space, which results in a minor change in accuracy when the wavelength of light is changed slightly.

Furthermore, we have analyzed and compared the widely used light sources employed in different related literature to see which pair performs the best among them when HbA1c and SpO_2 are estimated. The commonly used light wavelengths are derived from related studies, which include 465nm, 525nm, 593nm, 611nm, 660nm, and 950nm, respectively. Table 2 enlists the performance of different sets of wavelengths.

In Table 2, the bold typed numbers indicate the best performing set of wavelengths and the green fill-colored grids indicate the top five best performing sets of wavelengths that perform better than other sets of wavelengths for each corresponding model. From this table, it can be seen that the wavelength set {465, 525, 660} (blue, green, red) performs best among all the models. Other notable set of wavelengths include {465, 593, 660}, {465, 611, 660}, {465, 660, 950}, and {525, 660, 950}. Here, the 593nm, 611nm, and 950nm indicate yellow, orange, and infra-red, respectively.

With the results described above, we have implemented several models to estimate HbA1c and SpO_2 values using wavelengths close to 465nm, 525nm, and 660nm. In [7], [17] we performed different model based approaches to estimate HbA1c and SpO_2 values. All of the models exhibit greater accuracy compared to the state-of-the-art algorithms and processes on noninvasive glycated hemoglobin estimation. In these studies, the Beer-Lambert blood-vessel model and whole-finger models exhibited Pearson's R values of 0.92 and 0.96, respectively. Whereas, the photon diffusion transmission and reflection models resulted in Pearson's R values of 0.898 and 0.927, respectively.

On the other hand, in [20] we compared

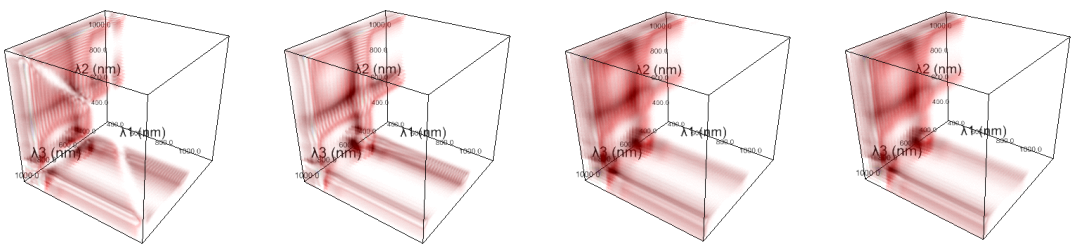

Fig. 1. Illustration of the value of M_h at a set of three different wavelengths (λ_1, λ_2, and λ_3) (in nm units) for (a) Beer-Lambert blood-vessel, (b) Beer-Lambert whole-finger, (c) Photon-diffusion transmission, and (d) Photon-diffusion reflection models. The intensity of red color in the figures indicates the higher value of M_h for that specific set of three wavelengths (λ_1, λ_2, λ_3). The data points have no units.

Table 2. Table of calculated M_h and M_s parameters' values for all combinations of widely used wavelengths for all Beer-Lambert and photon diffusion models.

Set of Wavelengths (λ_1, λ_2, λ_3) (nm)	Beer-Lambert Model				Photon Diffusion Model			
	Blood-Vessel		Whole-Finger		Transmission		Reflection	
	M_h	M_s	M_h	M_s	M_h	M_s	M_h	M_s
{465, 525, 593}	0.038	0.011	0.039	0.011	0.033	0.008	0.039	0.009
{465, 525, 611}	0.385	0.039	0.451	0.046	0.302	0.028	0.366	0.034
{465, 525, 660}	**1.471**	**0.168**	**2.896**	**0.462**	**1.147**	**0.118**	**1.44**	**0.152**
{465, 525, 950}	0.451	0.024	0.497	0.024	0.687	0.019	0.814	0.024
{465, 593, 611}	0.274	0.032	0.319	0.037	0.223	0.023	0.269	0.028
{465, 593, 660}	1.006	0.12	1.98	0.32	0.818	0.086	1.017	0.11
{465, 593, 950}	0.277	0.032	0.305	0.033	0.457	0.027	0.533	0.033
{465, 611, 660}	0.997	0.125	1.832	0.297	0.791	0.087	1.008	0.114
{465, 611, 950}	0.486	0.039	0.546	0.043	0.569	0.03	0.693	0.037
{465, 660, 950}	1.034	0.109	1.852	0.277	0.995	0.076	1.254	0.099
{525, 593, 611}	0.250	0.02	0.29	0.024	0.203	0.015	0.232	0.017
{525, 593, 660}	0.906	0.083	1.76	0.251	0.736	0.063	0.869	0.076
{525, 593, 950}	0.267	0.041	0.296	0.043	0.429	0.039	0.473	0.048
{525, 611, 660}	0.875	0.083	1.585	0.221	0.69	0.061	0.827	0.074
{525, 611, 950}	0.453	0.042	0.51	0.046	0.522	0.039	0.6	0.046
{525, 660, 950}	0.926	0.088	1.624	0.224	0.886	0.07	1.05	0.085
{593, 611, 660}	0.264	0.017	0.501	0.059	0.252	0.017	0.269	0.018
{593, 611, 950}	0.134	0.033	0.15	0.035	0.184	0.035	0.185	0.04
{593, 660, 950}	0.252	0.038	0.48	0.08	0.297	0.039	0.308	0.043
{611, 660, 950}	0.083	0.016	0.134	0.025	0.093	0.019	0.099	0.02

multi-wavelength models for accurately estimating HbA1c values. In that study, we compared two-wavelength and three-wavelength based models for getting the most accurate model to estimate HbA1c values. That study also used wavelengths closer to 465nm, 525nm, and 660nm.

Ⅳ. Conclusion

In this research, we have compared different wavelengths of light to analyze four different models based on Beer-Lambert and photon diffusion theories to deduce the best set of wavelengths that can estimate the glycated hemoglobin (HbA1c) and blood oxygenation (SpO_2) parameters accurately in a noninvasive manner.

First, we have conducted tests on these models for 300nm to 1100nm wavelengths of light and found that the set of 426nm, 721nm, and 1100nm wavelengths of light perform best for the Beer-Lambert blood-vessel model. On the other hand, 426nm, 678nm, and 1100nm light wavelengths are found best for the Beer-Lambert whole-finger model. Furthermore, for both of the photon diffusion models, the set of 426nm, 384nm, and 1100nm are found best performing among all the possible combinations of wavelengths.

We have also seen that among all the four models described here, the Beer-Lambert based model is seen to have a high slope of M_h values with the slightest change in wavelengths in operation. This is a drawback of the Beer-Lambert model, as the change of wavelengths due to change in temperature of fabrication defect, in hardware implementation can vary the accuracy of HbA1c and SpO_2 estimation heavily.

Finally, we have compared the performance of the six widely used wavelengths of light for all the Beer-Lambert and photon diffusion models and found that the set consisting 465nm, 525nm, and 660nm (blue, green, and red) performs the best among all the other combinations. The other notable combinations of wavelengths include {465, 593, 660}, {465, 611, 660}, {465, 660, 950}, and {525, 660, 950}.

References

[1] T. Tamura, Y. Maeda, M. Sekine, and M. Yoshida, "Wearable Photoplethysmographic sensors-past and present," *Electronics*, vol. 3, no. 2, pp. 282-302, Jun. 2014, doi: 10.3390/electronics3020282.

[2] P. P. Banik, S. Hossain, T.-H. Kwon, H. Kim, and K.-D. Kim, "Development of a wearable reflection-type pulse oximeter system to acquire clean PPG signals and measure pulse rate and SpO2 with and without finger motion," *Electronics*, vol. 9, no. 11, Art. no. 11, Nov. 2020, doi: 10.3390/electronics9111905.

[3] S. Rajala, H. Lindholm, and T. Taipalus, "Comparison of photoplethysmogram measured from wrist and finger and the effect of measurement location on pulse arrival time," *Physiol. Meas.*, vol. 39, no. 7, p. 075010, 2018, doi: 10.1088/1361-6579/aac7ac.

[4] K. Budidha, V. Rybynok, and P. A. Kyriacou, "Design and development of a modular, multichannel photoplethysmography system," *IEEE Trans. Instrumentation and Meas.*, vol. 67, no. 8, pp. 1954-1965, Aug. 2018, doi: 10.1109/TIM.2018.2810643.

[5] G. D. Jindal, T. S. Ananthakrishnan, R. K. Jain, V. Sinha, A. R. Kini, and A. K. Deshpande, "Non-invasive assessment of blood glucose by photo plethysmography," *IETE J. Res.*, vol. 54, no. 3, pp. 217-222, May 2008, doi: 10.1080/03772063.2008.10876202.

[6] S. Sen Gupta, T.-H. Kwon, S. Hossain, and K.-D. Kim, "Towards non-invasive blood glucose measurement using machine learning: An all-purpose PPG system design," *Biomed. Sign. Process. and Contr.*, vol. 68, p. 102706, Jul. 2021, doi: 10.1016/j.bspc.2021.102706.

[7] S. Hossain, S. S. Gupta, T.-H. Kwon, and K.-D. Kim, "Derivation and validation of gray-box models to estimate noninvasive in-vivo percentage glycated hemoglobin using digital volume pulse waveform," *Scientific Reports*, Jun. 2021, doi: 10.1038/s41598-021-91527-2.

[8] M. Shamir, L. A. Eidelman, Y. Floman, L. Kaplan, and R. Pizov, "Pulse oximetry plethysmographic waveform during changes in blood volume," *Br. J. Anaesth.*, vol. 82, no. 2, pp. 178-181, Feb. 1999, doi: 10.1093/bja/82.2.178.

[9] A. Temko, "Accurate heart rate monitoring during physical exercises using PPG," *IEEE Trans. Biomed. Eng.*, vol. 64, no. 9, pp. 2016-2024, Sep. 2017, doi: 10.1109/TBME.2017.2676243.

[10] H. Chang, et al., "A method for respiration rate detection in wrist PPG signal using holo-hilbert spectrum," *IEEE Sensors J.*, vol. 18, no. 18, pp. 7560-7569, Sep. 2018, doi: 10.1109/JSEN.2018.2855974.

[11] K. H. Shelley, "Photoplethysmography: Beyond the calculation of arterial oxygen saturation and heart rate," *Anesth. Analg.*, vol. 105, no. 6, pp. S31-36, Dec. 2007, doi: 10.1213/01.ane.0000269512.82836.c9.

[12] M. Kachuee, M. M. Kiani, H. Mohammadzade, and M. Shabany, "Cuffless blood pressure estimation algorithms for continuous health-care monitoring," *IEEE Trans. Biomed. Eng.*, vol. 64, no. 4, pp. 859-869, Apr. 2017, doi: 10.1109/TBME.2016.2580904.

[13] S. Mandal and M. O. Manasreh, "An In-Vitro optical sensor designed to estimate glycated hemoglobin levels," *Sensors* (Basel), vol. 18, no. 4, Apr. 2018, doi: 10.3390/s18041084.

[14] D. Shao, et al., "Noncontact monitoring of blood oxygen saturation using camera and dual-wavelength imaging system," *IEEE Trans. Biomed. Eng.*, vol. 63, no. 6, pp. 1091-1098, Jun. 2016, doi: 10.1109/TBME.2015.2481896.

[15] S. Hossain and K.-D. Kim, "Estimation of molar absorption coefficients of HbA1c in near UV-Vis-SW NIR light spectrum," in *Proc. KICS Fall Conf.*, pp. 208-209, Nov. 2020.

[16] S. A. Prahl, *Tabulated molar extinction coefficient for hemoglobin in water* (1998),

Retrived Aug., 01, 2019, from https://omlc.org /spectra/hemoglobin/summary.html.

[17] M. S. Hossain, *Glycated hemoglobin estimation based on photon diffusion theory*, M.S. Thesis, Kookmin University, Seoul, Korea, 2020.

[18] J. M. Schmitt, "Simple photon diffusion analysis of the effects of multiple scattering on pulse oximetry," *IEEE Trans. Biomed. Eng.*, vol. 38, pp. 1194-1203, 1991, doi: 10.1109/10.137285.

[19] R. J. Fretterd and R. L. Longini, "Diffusion dipole source," *J. Opt. Soc. Am., JOSA*, vol. 63, no. 3, pp. 336-337, Mar. 1973, doi: 10.1364/JOSA.63.000336.

[20] S. Hossain, C. A. Haque, and K.-D. Kim, "Quantitative analysis of different multi-wavelength PPG devices and methods for noninvasive In-Vivo estimation of glycated hemoglobin," *Applied Sci.*, vol. 11, no. 15, Art. no. 15, Jan. 2021, doi: 10.3390/app11156867.

시팟 호세인 (Shifat Hossain)

2017년 : Khulna University of Engineering and Technology (KUET) 전자공학과 학사
2021년 2월 : 국민대학교 전자공학과 석사
2021년 3월~현재 : 국민대학교 전자공학과 연구원
<관심분야> 디지털통신, 디지털신호처리
[ORCID:0000-0002-4537-2620]

김 기 두 (Ki-Doo Kim)

1980년 : 서강대학교 전자공학과 학사
1980년~1985년 : 국방과학연구소 연구원
1988년 : 미국 펜실베니아 주립대학교 전자공학 석사
1990년 : 미국 펜실베니아 주립대학교 전자공학 박사
1998년~1999년 : 미국 UCSD, Visiting Scholar
1991년~현재 : 국민대학교 전자공학부 교수
<관심분야> 디지털통신, 디지털신호처리
[ORCID:0000-0001-5052-3844]